www.sciencemag.org/cgi/content/full/335/6066/324/DC1

Supporting Online Material for

Destruction of Sun-Grazing Comet C/2011 N3 (SOHO) Within the Low Solar Corona

C. J. Schrijver,* J. C. Brown, K. Battams, P. Saint-Hilaire, W. Liu, H. Hudson, W. D. Pesnell

*To whom correspondence should be addressed. E-mail: schrijver@lmsal.com

Published 20 January 2012, *Science* **335**, 324 (2012)
DOI: 10.1126/science.1211688

This PDF file includes:

Additional online material includes the following:

Movies S1 and S2

Supporting online material

S1: EUV movies of the comet streaking across the Sun

The first movie (S1) shows cutouts of images taken by the Atmospheric Imaging Assembly onboard the Solar Dynamics Observatory using its 171 Å channel (designed to observe emission from Fe^{8+} and Fe^{9+} ions, emitting around 1 MK). The images were taken at a cadence of 12 s; an unsharp-mask operation was used to enhance the contrast (courtesy of T. Berger, LMSAL). A second movie (S2) shows cutouts (without spatial filtering) that move (in full pixel steps) with the position of the comet, located at the center of the circle. The comet's positions were measured as the approximate head of the EUV-bright tail, then fit by a parabola to derive a smooth trajectory, used to extrapolate beyond the time of clear visibility. The tail is very faintly visible from the moment the comet enters the AIA field of view; neither bright tail nor dark coma are seen with AIA past the last determined position at 2011/07/06 00:05:50 UTC. The time stamp also shows the elapsed time in seconds since the t_0 at 2011/07/05 23:40:01 UTC. Asterisks in the top-right corner in the frames mark times of maximum brightness in Fig. 3.

S2: Coma in absorption

Fig. S1 shows the intensity profiles of the comet's head and tail, corrected for the background intensity measured 36 s before the comet's arrival at those positions, for the 131, 171, 193, and 211 Å channels for a cut along the center line of the comet's tail, expressed relative to the background intensity. The negative values at -5000 km are caused by the absorption in the denser inner region of the comet's coma immediately surrounding the nucleus or cluster of residual nuclei.

To achieve an intensity reduction of approximately 2% over the 7 pixel area over which the signal is averaged, requires an opaque area of $\approx 3 \times 10^{14}$ cm^2. In S3 we estimate a mass-loss rate from the comet of $\dot{m} = 10^6 - 10^8$ g/s, decelerating behind the nucleus into the coronal rest frame through the EUV-bright tail with a length of approximately 15,000 km. Assuming a constant rate of deceleration, it would take the mass approximately 10 s to fall behind a coma with effective radius of 700 km (see S3 for the origin of these estimates). For gas with a high water vapor content (with atomic mass μ; or within a factor of two for a high oxygen content after dissociation of the water molecules), for example, this would imply a mean column density within the coma of $\dot{m}/(\mu \pi r_c^2 = 3 \times 10^{13} - 3 \times 10^{15}$ cm^{-2}, which would absorb (*17*) $\approx 0.015 - 1.5\%$ of the EUV signal. This is consistent with the observed EUV attenuation for values at the high end of the mass loss rate estimated in S3.

S3: Mass estimate from tail deceleration

In order for the released cometary material to decelerate through the tail along the comet's direction of motion through the corona, it must interact and exchange momentum with the surrounding coronal plasma that it is moving through. Using the conservation of the kinetic energy of the large-scale motion through the coronal

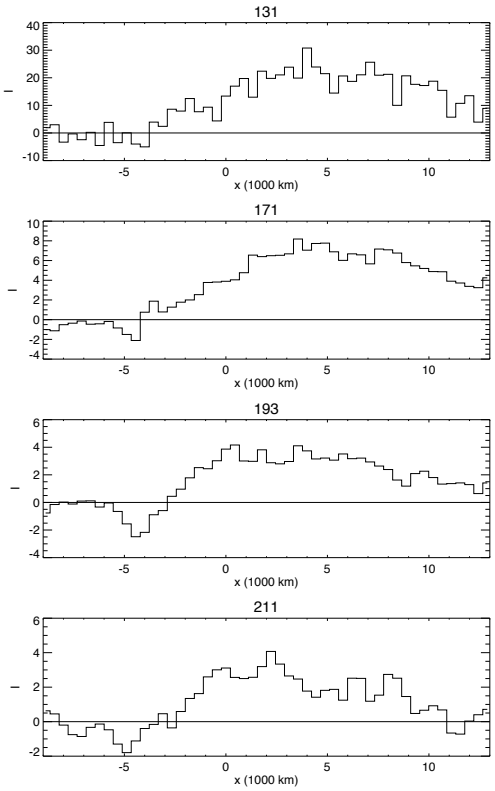

Figure S1: *Relative intensity profiles, expressed in percent, of the comet's head and tail for the 131, 171, 193, and 211 Å channels measured around the time of the limb crossing (averaging over images taken between 23:50:00 UT and 23:53:24 UT) when the coma's absorption is most pronounced. These profiles are averaged intensity profiles of running-difference images relative to the background intensity in the same positions 36 s earlier, as shown in Fig. 4, collapsed between 600 to 800 s past the reference time defined in Fig. 4.*

environment and the associated linear momentum conserved in the collisions between the cometary material and the closed-field coronal plasma (the comet does not probe the solar wind in its final phase, see Fig. 1),

$$v_n \dot{m}_n = v_c \dot{m}_c + a v_n \dot{m}_n, \quad (1)$$

$$\frac{1}{2}\dot{m}_n v_n^2 = \frac{1}{2}\dot{m}_c v_c^2 + \frac{1}{2}\dot{m}_n a^2 v_n^2, \quad (2)$$

where the comet mass lost per unit time $\dot{m}_n$ from the nucleus must collide with coronal plasma swept by per unit time with mass $\dot{m}_c$, rebounding via collisions and the Lorentz force to a final velocity v_c with respect to the ambient corona; a is the ratio of post-deceleration velocity to the relative orbital velocity v_n of the

comet's nucleus. From the above conservation equalities, we find that

$$\dot{m}_n = \frac{1-a^2}{(1-a)^2}\dot{m}_c, \tag{3}$$

implying, for small values of a, that the mass sublimated per second must collide with about the same mass to decelerate substantially.

The coronal mass with which the cometary mass interacts at any given time interval while slowing down is given by the integration of the density through the volume of the comet's tail

$$m_c = \pi r_{coma}^2 \ell_t n_c m_p, \tag{4}$$

for an effective radius of the coma of r_{coma} (within which most of the material is contained), slow-down path length in the tail of ℓ_t, and proton mass m_p. The ambient coronal density of n_c within the roughly isothermal quiet-Sun corona can be approximated by $n_c = n_o exp(-h/H)$, for a base ion density of $n_0 = 5\times10^8$ cm^{-3} (*10*), height h, and pressure scale height $H = 75000$ km for a plasma temperature of 1.5 MK.

The mass m_c interacts with tail material within the time $\tau_t \approx 2\ell_t/v_n$ that it takes for the comet's mass to move through the tail (at an average speed of half the nucleus' orbital velocity, v_n, which is close to 600 km/s) and come nearly to rest within the ambient corona. With $\dot{m}_c = m_c/\tau_t$ (in which the tail length cancels out), combination with Eqs. (3) and (4) yields a characteristic mass-loss rate for the nucleus during its visibility in the AIA observations of

$$\dot{m}_n \approx \frac{1-a^2}{(1-a)^2}\pi r_{coma}^2 n_0 m_p \frac{v_n}{2} \exp\left(-h/H\right) = (0.01-1)\times10^8 \mathrm{g/s} \tag{5}$$

for $r_{coma} = 50-700$ km, an average height of $h = 120$ Mm, and with $a = 1/6$ to bring the velocity down to 100 km/s at the end of the EUV-bright tail (the results differ by less than a factor of two for $a < 1/3$). This phase of the demise of the comet lasts for about 10 minutes, during which a total mass of $(0.06-6)\times10^{10}$ g is lost. The uncertainty range is dominated by the uncertainty in the coma's size, given estimated uncertainties in n_0 of 50% and in the pressure scale height H of ≈ 20 Mm (resulting from the range of temperatures in the quiet-Sun corona). The comet's orbit is known so well that uncertainties in that value are a relatively small contribution to the total uncertainty.

We note that the diameter of the nuclear bodies (of order $10-50$ m and less at the start of this phase of visibility with SDO/AIA; see S4) is very much smaller than even the dense EUV-absorbing part of the coma, so that no measurable deceleration of the nucleus should occur as a result of its interaction with the coronal plasma.

These estimates for mass loss rate and total mass lost assume that the comet's material is completely sublimated and that all material is decelerated with the component visible in the AIA images; if part of the mass should survive in the form of dust for more than a few minutes in the intense radiation field from the solar surface, for example, then these estimates serve as lower limits.

In the above derivation, we have ignored the role of the coronal magnetic field. In order for the magnetic field to have an effect on matter, the latter must be mostly ionized. As matter initially sublimates from the nucleus, this is not the case: the vast bulk of the photons in the solar radiation field at an effective temperature of $T \approx 5800\,\mathrm{K}$ are not energetic enough to result in a substantial ionization of the atoms lost from the nuclear volume, although it will be effective in dissociating molecular compounds. Bulk ionization for this case requires that most atoms collide with the coronal plasma. Once that has occurred, the magnetic field may indeed have a grip on the comet's tail, but this leaves the above estimates for mass loss rate and total mass lost largely valid.

Once ionization has occurred, the ions in the cometary tail and the coronal magnetic field become coupled. But initially, that coupling does not do much to impede the motion of the material in the tail; on the contrary, that material appears to have enough momentum at first to deform the magnetic field. We can estimate the relative effect of the coronal field on the mass lost from the comet by computing an effective plasma-β as the ratio of the kinetic energy density in the mass lost from the nucleus relative to the energy density in the magnetic field (estimated to be between 0.4 G and 0.8 G from the PFSS model shown in Fig. 1a):

$$\beta_{\mathrm{eff}} = \frac{\frac{1}{2}\rho v_{\mathrm{n}}^2}{B^2/8\pi} = \frac{\dot{m}_n v_{\mathrm{n}}}{r_{\mathrm{coma}}^2 B^2} \gtrsim 4 \tag{6}$$

for the mass loss rate $\dot{m}_n$ from Eq. (5); the range of values is dominated by the range in field strengths as the comet descends through the corona and is independent of the estimate of the radius of the coma. Conservatively, our observations only give a wide range between lower and upper limits for the radius of the primary or any major fragment. This estimate shows that the field is not strong enough to guide the motion of the cometary tail until the latter has decelerated substantially. The observations (S1) are consistent with this, revealing limited northward deflection of the tail.

S4: Mass estimate from insolation sublimation

At heights exceeding $0.01\,R_\odot$ or 70,000 km above the solar photosphere, mass loss is dominated by insolation sublimation, where the surface layers evaporate into space as they absorb the incident solar radiative energy (*3*, *6*). This produces a sublimation timescale of order 0.2 s times the initial size in cm, or 10^3 – 10^4 s for $m = 10^9 - 10^{12}$ g (10-100 m in characteristic size) (*6*). The time of final disappearance is thus a direct measure of the mass.

During the terminal phase of comet C/2011 N3, the value $\mathcal{F}$ of the insolation can be taken to be a constant 4.4×10^{10} ergs/cm^2/s. The mass sublimated from a comet nucleus subject to insolation is then estimated by

$$\begin{aligned} \frac{dm}{dt} &= -\frac{d^2\mathcal{F}}{\mathcal{L}} = -\frac{m^{2/3}\mathcal{F}}{\rho^{2/3}\mathcal{L}} \equiv -bm^{2/3} \\ m(t) &= \left(m(t=0)^{1/3} - \frac{1}{3}bt\right)^3 \end{aligned} \tag{7}$$

(see Brown *et al*. (*6*) and earlier work by, e.g., (*2, 18, 19*)), for mean diameter d, incoming flux $\mathcal{F}$, latent heat for vaporization $\mathcal{L}$, and mean mass density ρ. For a value of $\mathcal{L} = (3-8) \times 10^{10}$ erg/g, covering the "normal" cometary composition of water ice and asteroidal material, and a density of $\rho = 0.6 \pm 0.2$ g/cm^3 (see the discussion and references in Brown et al. (*6*) going back to, e.g., (*18,19*), we have $b \approx 1.1 \pm 0.5$ g$^{1/3}$/s.

To compare with the mass estimates from the EUV observations only the mass lost during the terminal phase of the comet is considered here. Using a 1300 s interval for this phase (final sublimation of the nucleus determined by the time of the last detection in the STEREO/EUVI images) in Eq. (7) yields a mass estimate of 10^8 g. That mass estimate lies one to three orders of magnitude below the estimate presented in S3 based on the observed deceleration. Yet in S5, we argue that that higher mass estimate is needed to understand the brightness of the comet's tail in the AIA images. This mismatch may point to not a single body but rather a distribution of sizes of cometary fragments, which increases the total area and thus the insolation power relative to the total latent energy of sublimation.

The size distribution of Kreutz comet nuclei larger than 5 m has been shown to be a power law (*2*):

$$N(r)dr = \alpha r^{-\gamma} dr, \tag{8}$$

with a best-fit power law index of $\gamma \approx 3.2$, somewhat shallower and rich in larger bodies than the Dohnyani collisional equilibrium (*20*) with a power-law index of 3.5. We do not know the distribution of fragment sizes for C/2011 N3, but let us assume that this general size distribution holds for the observed object throughout its demise by insolation.

We set the value of γ to 3 below as this enables a compact expression with adequate fidelity. With such a power-law distribution, the total mass and total mass-loss rate can be readily computed given a range of fragment radii from r_0 to r_1:

$$m = \frac{\alpha 4\pi\rho}{3}(r_1 - r_0); \tag{9}$$

$$\frac{dm}{dt} = \frac{\alpha\pi\mathcal{F}}{\mathcal{L}} \log(r_1/r_0). \tag{10}$$

For an average mass-loss rate $dm/dt \approx m/t_{\rm EUV}$ for the time interval $t_{EUV} \approx 600$ s over which the comet's tail is bright in EUV, we obtain the following expressions for the upper limit of the mass derived in S3:

$$\alpha r_1 = 2.6 \times 10^{10}\,;\, \alpha \log(r_1/r_0) = 4.3 \times 10^7. \tag{11}$$

The resulting values for α and r_1 are only logarithmically dependent on the ratio r_1/r_0. If we set $r_1/r_0 \approx 100$, then $\alpha \approx 10^7$, and $r_1 \approx 30$ m; for $r_1/r_0 \approx 10^4$, for example, we find $\alpha \approx 5 \times 10^6$, and $r_1 \approx 55$ m . With that range of values of α, the total number of nuclear objects with sizes exceeding, say, 5 m (for which the size distribution of Kreutz family nuclei was established (*2*)) is $\approx 10 - 20$. In view of the assumptions made above, some with substantial uncertainties, these are reasonable numbers; sublimation-driven fragmentation may also help us understand the intrinsic EUV variability of the comet's tail shown in Fig. 3.

S5: Mass estimate from EUV brightness of the tail

The mechanism that excites the ions responsible for the emission from the EUV-bright comet tail remains to be established. Direct insolation by solar radiation can readily be excluded: the effective temperature of the solar radiation field is 5780 K, which suffices to evaporate cometary solids and lightly ionize them but is insufficient to warm the comet's material to a level where the glow would be observable at EUV wavelengths. The coronal EUV radiation field would eventually heat up the material, but that would take far too long (the total coronal X-ray and EUV emission is 5 to 6 orders of magnitude less than the solar luminosity of $\approx 4 \times 10^{33}$ ergs/s).

We consider three candidate excitation mechanisms, from which mass-loss estimates or upper limits to that mass loss can be established by somewhat parallel arguments: (a) direct collisional excitation, (b) electron heat conduction into the tail from the embedding corona, and (c) charge-exchange collisions.

We first consider (a): direct collisional excitation (with about 2 keV/nucleon available in the comet's kinetic energy when moving at ≈ 600 km/s through the corona), which allows us to set a lower limit on the mass-loss rate from the nucleus by comparing the brightness of the comet's tail to that of the background corona, using a ratio of estimated emission measures.

An upper limit to the emission measure for the heavy-element rich cometary tail can be achieved as follows. The material lost by insolation of the nucleus moves through the tail at an average velocity of $< v > \approx 300$ km/s at a mean particle density n_t that is found with Eq. (5) for a value of $r_{\rm coma}$ that we here set to the high end of its range, i.e., ≈ 700 km (we return to this below):

$$n_t = \frac{\dot{m}_n}{\pi r_{\rm coma}^2 < v > \mu m_{\rm p}} = \frac{1}{\mu} 1.5 \times 10^8 \, {\rm cm}^{-3}, \tag{12}$$

where this number density is expressed using the average nuclear mass $\mu m_{\rm p}$ to allow for the comet's composition, which is poor in the hydrogen and helium that dominate the solar plasma but but rich in elements of high atomic numbers (such as C, O, Mg, Si, Fe, S, etc.) that can easily provide electrons to the coronal plasma.

The equivalent column emission measure (for the moment ignoring the ionization state of the plasma by putting that into a combined factor $\alpha\gamma$) is

$$EM_t = (\gamma n_{\rm i})(\alpha n_{\rm e}) 2 r_{\rm coma} = \frac{\alpha\gamma}{\mu^2} 3 \times 10^{24} \, {\rm cm}^{-5}. \tag{13}$$

Here, α is a correction factor to allow for the fact that the coma material yields many more electrons per atom than the atoms in the hydrogen-helium dominated coronal plasma. If the emission in the AIA EUV channels is dominated by the iron lines to which the channels are tuned, then the factor γ is the iron abundance in the comet relative to the solar coronal iron abundance.

The above result can be compared to the line-of-sight integrated emission measure in the approximation of an isothermal corona (at about 1.5 MK averaged over the quiet Sun) at a base density of $n_0 = 5 \times 10^8$ cm^{-3} (*10*) and density scale height $H \approx 75000$ km. The column emission measure, for ion and electron densities $n_{\rm i,e}$, is then

$$EM_c = \int_0^\infty n_i n_e dh/cos(\theta) \;\; = \;\; \int_0^\infty \left(n_0 \exp\left(-h/H\right)\right)^2 \, dh/cos(\theta)$$

$$= \frac{1}{2cos(\theta)} n_0^2 H \approx 1.8 \times 10^{27}\,\mathrm{cm}^{-5}, \quad (14)$$

where the factor $cos(\theta)$ accounts for the fact that the line of sight for the integration is not normal to the surface; we take $\theta = 60^\circ$ for the value given the observation conditions of C/2011 N3.

We thus find a ratio of brightnesses for the tail and coronal emissions of

$$\frac{EM_t}{EM_c} < \frac{\alpha\gamma}{\mu^2} 1.6 \times 10^{-3} \approx 0.06. \quad (15)$$

In the last numerical value we assumed $\gamma = 4 \times 10^2$, i.e., that iron represents about 1% of the comet's atoms as compared to about one in 4×10^4 as in the corona (which is equivalent to taking the abundances to be solar, but for H and He (*15*)). We further approximate the relative electron donor capacity per atom and the mean atomic mass compared to the solar coronal values at $\alpha \approx 10$ and $\mu \approx 10$.

The above estimate of a 6% contrast between the comet's tail brightness and that of the background quiet-Sun corona is of the same order of magnitude as the observed values for the coronal EUV channels of SDO/AIA (see Fig. 3), i.e., that the spectrum of the cometary tail and of the background corona are plausibly of the same shape. This estimate assumes the same ionization fractions, i.e., a temperature of about 1.5 MK for both plasmas.

This estimate shows that it is quantitatively possible for the tail to be emitting photons from collisionally ionized iron with ionization states characteristic of plasma somewhat below 1 MK. Yet this scenario provides a rather conservative lower-limit to the comet's mass-loss rate from the EUV brightness because the above value assumes that the ionization states are effectively brought to a level comparable to that of the background corona. These rough quantitative estimates are consistent only with the observed tail brightness if the total mass involved, and the coma's effective radius involved in that estimate, lie near the upper end of their range derived in S3.

Next, we consider (b) electron conduction as an efficient way to equilibrate the temperatures of the surrounding corona with that of the material being lost through the comet's tail. In this scenario, the collisionally ionized mixture of sublimated material would be brought to an ionization equilibrium that naturally matches that of the large thermal reservoir of the surrounding corona, so that the emission measure contrast given by Eq. (15) is rapidly brought to a value comparable to the observed intensity contrast. If we estimate the time scale for thermal conduction by comparing the thermal energy content $3nkT$ of the plasma within the tail with the rate at which classical Spitzer electron conduction transports energy across a thermal gradient:

$$\tau_\mathrm{e} \equiv \frac{3nkT}{F_C} \approx \frac{3nkT}{\kappa_\mathrm{c} T^{7/2}/\ell_\mathrm{c}^2}, \quad (16)$$

for a plasma being brought to ambient temperature T with tail density n, with a gradient length scale ℓ_c and using the standard Spitzer electron conductivity κ_c. For a temperature contrast of ≈ 1 MK, at the ambient density estimated above, and a length scale of order $\ell_\mathrm{c} \sim 1000$ km, we find τ_e to be on the order of a second.

The application of the Spitzer conductivity requires that $\ell_{\rm c}$ substantially exceeds the electron mean free path for ion-electron collisions,

$$\lambda_{\rm mfp} \approx 1.1 \times 10^3 \frac{T_6^2}{n_8} \frac{20}{\ln(\Lambda)} \,{\rm km} \tag{17}$$

for n_8 the density in units of $10^8\,{\rm cm}^{-3}$, T_6 the temperature in MK, and $\ln(\Lambda) \approx 10 - 20$ the Coulomb integral (*21*). In the case of the comet's tail, $\lambda_{\rm mfp}$ is of order 1500 km (using the density estimated above and with $T_6 \approx 1.5$), which is comparable to the diameter of the tail. A empirical correction (*21*) relating the achieved thermal conduction F_C^* to the classical Spitzer value F_C in this case is given by

$$F_C^* = 0.11 \left(\frac{\ell_{\rm c,8}}{\lambda_{\rm mfp}} \right)^{0.36} F_C \approx 0.1 \left(\frac{n_8 \ell_{\rm c,8}}{T_6^2} \right)^{0.36} F_C, \tag{18}$$

which for the tail's conditions is of order $0.1 F_C$, so that the time scale $\tau_{\rm e}$ becomes of order 10 s (roughly comparable to the estimated time for material to fall behind the nuclear material to the head of the EUV-bright tail).

Note that the ionization energies of Fe^{8+} and Fe^{9+}, which are the dominant ionization states at $\approx$ 1 MK, are naturally comparable to the thermal energy. Hence, it should take only seconds to tens of seconds to conduct enough energy into a tail of up to a few thousand kilometers in cross section to bring the atoms to ionization states characteristic of the temperature of the embedding coronal plasma.

Lastly, we consider mechanism (c): charge-exchange collisions. This mechanism is responsible for the X-ray and EUV signatures of comets far from the Sun where cometary neutrals interact with the ions in the solar wind (*12, 13*): ions coming within about 1 nm of a neutral atom or molecule capture an electron, which – if that ends up in a highly-excited state – results in the emission of relatively high-energy photons upon the subsequent de-excitation (often in a stepped cascade).

The neutrals sublimating away from the nucleus of C/2011 N3 (SOHO) will encounter the ionized material of the solar corona at the orbital velocity of 600 km/s, comparable to the relative velocities involved for the interaction of cometary neutrals with the solar wind far from the Sun, so the velocity-dependent cross sections used for interplanetary charge exchange analyses should be applicable here. In this scenario, the excited ions from which subsequent emission can be expected into the AIA passbands will be at most those involved in the collisional interaction with the cometary material, which is comparable to the estimated mass of the cometary gas streaming through the tail. Hence, Eq. (15) can be directly applied to estimate the emission measure ratio. In this case, however, the emitting tail plasma has, by definition, the solar coronal composition, so that $\alpha\gamma/\mu^2 = 1$, yielding $\frac{EM_t}{EM_c} \approx 1.6\,10^{-3}$, with is about 1.5 orders of magnitude too low to match the observed brightness. As the charge-exchange collisions leave the captured electrons in a range of orbital energies, that difference is in reality even larger, so that charge-exchange collisions appear less efficient than the two processes above.

We can illustrate the reason why deep in the solar corona charge-exchange collisions between cometary neutrals and coronal ions are likely less efficient as an

excitation mechanism leading to EUV emission than collisions between cometary ions and coronal electrons by directly comparing the total collision rates, C_{CX} and C_{ie}, respectively.

The rate of charge exchange collisions with atoms of species i with relative abundance A_i equals the total number of such atoms lost from the comet's nuclear bodies per second because each atom lost becomes a charged ion after a single interaction:

$$C_{CX} = \frac{\dot{m}}{\mu m_{\rm p}} A_i. \tag{19}$$

C_{ie} is the product of the ion-electron collision frequency per electron, ν_e, and the total number of ions contained within the tail, equal to the ion-loss rate from the nuclear bodies times the average dwell time of these atoms within the tail. Combining the mean free path estimate for electron-ion collisions in Eq. (17) with the electron thermal velocity of $v_e = 4.2 \times 10^7 T^{1/2}$ yields $\nu_e = 4 \times 10^3 n/T^{3/2}$, so that:

$$C_{ie} = \nu_e \frac{\dot{m}}{\mu m_{\rm p}} A_i \frac{2\ell_t}{v_n}. \tag{20}$$

Combining Eqs. (19) and (20) yields a collision rate ratio of

$$\frac{C_{ie}}{C_{CX}} = 4 \times 10^3 \frac{n}{T^{3/2}} \frac{2\ell_t}{v_n} \approx 2 \times 10^4. \tag{21}$$

This shows the total number of ion-electron collisions per second to very much larger than the number of ion-neutral charge-exchange collisions in the relatively dense environment of the solar corona (mainly because of the coronal density compared to the solar-wind density which is, for example, of order $3 - 10\,{\rm cm}^{-3}$ near Earth orbit). Ion-ion charge-transfer collision that occur after the initial ionization will cause the ratio R of electron-ion to ion/neutral-ion charge-transfer collisions to be lower than the expression in Eq. (21), but because the total number of collisional interactions between cometary atoms and coronal ions is limited to an average of a few dozen (as argued when analyzing the tail deceleration in S3, realizing that the cometary material is relatively heavy compared to the hydrogen-helium dominated coronal plasma), the electron-ion collision rate will exceed the charge-transfer collision rate by at least three orders of magnitude in any case.

References

1. G. E. Brueckner *et al*., The Large Angle Spectroscopic Coronagraph (LASCO). *Sol. Phys.* **162**, 357 (1995).

2. M. M. Knight *et al*., Photometric study of the Kreutz comets observed by SOHO from 1996 to 2005. *Astron. J.* **139**, 926 (2010).

3. M. Iseli, M. Küppers, W. Benz, P. Bochsler, Sungrazing comets: Properties of nuclei and in situ detectability of cometary ions at 1 AU. *Icarus* **155**, 350 (2002).

4. J. R. Lemen *et al*., *Sol. Phys.* 10.1007/s11207-011-9776-8 (2011).

5. R. A. Howard *et al*., Sun Earth Connection Coronal and Heliospheric Investigation (SECCHI). *Space Sci. Rev.* **136**, 67 (2008).

6. J. C. Brown, H. E. Potts, L. J. Porter, G. le Chat, http://arxiv.org/abs/1107.1857 (2011).

7. See supporting material on Science Online.

8. www.minorplanetcenter.net/mpec/K11/K11N41.html; MPEC 2011-N41: COMET C/2011 N3 (SOHO).

9. C. J. Schrijver, M. L. DeRosa, *Sol. Phys.* **212**, 165 (2003).

10. P. Boerner *et al*., *Sol. Phys.* 10.1007/s11207-011-9804-8 (2011).

11. M. Guhathakurta, R. R. Fisher, R. C. Altrock, Large-scale coronal temperature and density distributions, 1984-1992. *Astrophys. J.* **414**, L145 (1993).

12. At heights above 0.01 solar radii, collisional heating and ablative mass loss by atmospheric impacts are negligible (*6*).

13. T. E. Cravens, X-ray emission from comets. *Science* **296**, 1042 (2002).

14. C. M. Lisse, T. E. Cravens, K. Dennerl, in *Comets II*, M. C. Festou, H. U. Keller, H. A. Weaver, Eds. (Univ. of Arizona Press, Tucson, AZ, 2004), pp. 631–643.

15. A. Delsemme, The chemistry of comets. *Philos. Trans. R. Soc. London Ser. A* **325**, 509 (1988).

16. www.minorplanetcenter.net.

17. C. W. Allen, *Astrophysical Quantities* (Athlone/Univ. of London, London, 1972).

18. P. R. Weissman, Cometary impacts with the Sun: Physical and dynamical considerations. *Icarus* **55**, 448 (1983).

19. Z. Sekanina, Erosion model for the sungrazing comets observed with the Solar and Heliospheric Observatory. *Astrophys. J.* **597**, 1237 (2003).

20. J. S. Dohnanyi, Collisional model of asteroids and their debris. *J. Geophys. Res.* **74**, 2531 (1969).

21. R. Rosner, B. C. Low, T. E. Holzer, in *Physics of the Sun.* P. A. Sturrock, T. E. Holzer, D. M. Mihalas, R. K. Ulrich, Eds. (Reidel, Dordrecht, Netherlands, 1986), vol. 2, pp. 135–180.